Applied Energy 147 (2015) 74–81

Contents lists available at ScienceDirect

Applied Energy

journal homepage: www.elsevier.com/locate/apenergy

Electrochemical investigation of thermically treated graphene oxides as electrode materials for vanadium redox flow battery

O. Di Blasi, N. Briguglio, C. Busacca, M. Ferraro, V. Antonucci, A. Di Blasi *

CNR-Istituto di Tecnologie Avanzate per l'Energia "Nicola Giordano" (ITAE), Salita S. Lucia sopra Contesse, 5 – 98126 Messina, Italy

HIGHLIGHTS

- Graphene oxide is synthesized at high temperatures in a reducing environment.
- Treated graphene oxide-based electrodes are prepared by the wet impregnation method.
- Electrochemical performance is evaluated as a function of the physico-chemical properties.

ARTICLE INFO

Article history:
Received 5 December 2014
Received in revised form 20 February 2015
Accepted 22 February 2015
Available online 12 March 2015

Keywords:
Vanadium redox flow battery
Thermically treated graphene oxides
Wet impregnation method
Electrochemical properties

ABSTRACT

Thermically treated graphene oxides (TT-GOs) are synthesized at different temperatures, 100 °C, 150 °C, 200 °C and 300 °C in a reducing environment (20% H_2/He) and investigated as electrode materials for vanadium redox flow battery (VRFB) applications. The treated graphene oxide-based electrodes are prepared by the wet impregnation method using carbon felt (CF) as support. The main aim is to achieve a suitable distribution of the dispersed graphene oxides on the CF surface in order to investigate the electrocatalytic activity for the VO^{2+}/VO_2^+ and V^{2+}/V^{3+} redox reactions in the perspective of a feasible large area electrodes scale-up for battery configuration of practical interest. Cyclic voltammetry (CV) and electrochemical impedance spectroscopy (EIS) are carried out in a three electrode half-cell to characterize the electrochemical properties of the TT-GO-based electrodes. Physico-chemical characterizations are carried out to corroborate the electrochemical results. The TT-GO sample treated at 100 °C (TT-GO-100) shows the highest electrocatalytic activity in terms of peak to peak separation (ΔE = 0.03 V) and current density intensity (~0.24 A cm^{-2} at 30 mV/s) both toward the VO^{2+}/VO_2^+ and V^{2+}/V^{3+} redox reactions. This result is correlated to the presence of hydroxyl (—OH) and carboxyl (—COOH) species that act as active sites. A valid candidate is individuated as effective anode and cathode electrode in the perspective of electrodes scale-up for battery configuration of practical interest.

1. Introduction

Electrical Energy Storage (EES) plays a key role to improve the whole power system due to the growing integration of renewable energy sources into the existing electricity grid [1,2]. Reliability and power quality, load levelling, spinning reserve, back start and reduced fuel use represent just few of the several benefits due to the integration of electricity storage into the grid [1,3–10]. Lithium-ion (Li-ion), Sodium Sulfur (NaS) and redox flow batteries (RFBs) are promising large-scale storage technologies due to their high performance, long cycle life and high efficiency [9–16]. In particular, Vanadium redox flow battery (VRFB) has been receiving great interest due to the cell configuration flexibility [17] and the reduced issue related to the cross-mixing of the anodic and cathodic vanadium electrolytes [18,9,19,20]. In literature, several works are addressed toward materials and components optimization [19,21–28] to improve the battery electrochemical performance. The membrane-electrode-assemblies (MEAs) constitute the active part of each single cell in which the redox reaction occurs [19,21–23]. Typically carbon-based electrodes, such as carbon paper, graphite felt, carbon felt and carbon cloth are the most common utilized materials for VRFB applications [9,17,21,22]. Due to the poor kinetic reversibility, chemical and thermal treatments are investigated to increase the electrochemical performance by modifications in terms of oxygen functional groups content [19,22,24]. Recently, graphene-based materials are investigated as a promising electrode materials for energy storage/generation device due to its surprising physico-chemical behaviors. Graphene, one-atom-thick two-dimensional layers of sp^2-bonded

* Corresponding author. Tel.: +39 090624281; fax: +39 090624237.
E-mail address: diblasi@itae.cnr.it (A. Di Blasi).

http://dx.doi.org/10.1016/j.apenergy.2015.02.073
0306-2619/

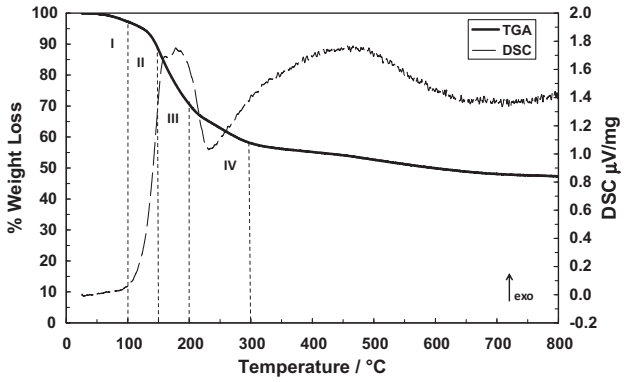

Fig. 1. TG/DSC curve of the graphene oxide (GO) powder in 20% H_2/He atmosphere.

carbon, is characterized by very high electrical and thermal conductivity, mechanical stiffness, and a high electrochemical activity [23] that make it highly attractive for many applications such as super-capacitors, Li-ion batteries, solar cells and fuel cell [29–31]. To the best of our knowledge few scientific works are addressed toward the electrochemical investigation of graphene and graphene oxides, obtained starting from graphite thermal treatment, by using noble metal foils or glassy carbon as support finalized to materials electrochemical study for VRFB [32,33]. Furthermore, no scientific works are addressed toward the study of the electrochemical performance of graphene oxides treated at high temperatures in a reducing environment for VRFB applications. Our study is an in-depth investigation of in-house thermically treated graphene oxide electrochemical properties as a function of the oxygen functional groups presence by developing electrodes prepared by wet impregnation method. This simple and practical technique consists in the carbon felt (CF) impregnation, used as support, by treated graphene oxide powders dispersed in an appropriate solvent. A whole covering of the carbon fiber of the support guarantees a suitable distribution of the TT-GOs on the CF surface area allowing the investigation of the electrochemical performance for the VO^{2+}/VO_2^+ and V^{2+}/V^{3+} redox reactions at the electrode-electrolyte interface. Moreover, the carbon felt structure allows to ensure both a mechanical resistance and an appropriate as well as stable electric contact between electrode and the terminal plate representing fundamental aspects in the perspective of a large area MEA scale-up for a battery configuration.

Table 1
Full width at half maximum (FWHM) and interlayer distance (d-spacing) of the investigated samples.

Samples	FWHM (°)	d-spacing (Å)
GO	1.073	8.61
TT-GO-100	0.968	8.50
TT-GO-150	2.504	7.61
TT-GO-200	5.109	3.78
TT-GO-300	5.873	3.74

1.1. Outline of the paper

The outline of the paper is as follow: Section 2 will give information about materials and methods utilized to prepare the several investigated samples. In Section 3.1, physico-chemical properties of the samples will be in depth evaluated by X-ray diffraction analysis, X-ray photoelectron spectroscopy and Fourier-transform infrared spectroscopy. In Section 3.2, electrochemical characterizations will be carried out on the investigated samples to corroborate results reported in the previous Section. Conclusions, about the obtained experimental data, are reported in Section 4.

2. Materials and methods

2.1. Thermically treated graphene oxides synthesis

A commercial graphene oxide (GO, Graphenea 4 mg/ml) was thermically treated at different operative temperatures in a reducing environment in order to synthesize several treated graphene oxides. A commercial GO volume (100 ml) was dried by an heating plate at 50 °C to obtain a GO sample in powder form. Thermal gravimetry and differential scanning calorimetry analyses (TG/DSC, STA 409C NETZSCH-Gerätebau GmbH Thermal Analyse) were carried out on the commercial GO powder from room temperature up to 800 °C at a heating rate of 5 °C/min in 20% H_2/He atmosphere. According to the main weight sample losses observed by TG analysis, thermal treatment temperatures were selected for the samples synthesis. Then, several GO powders were separately treated for 30 min at the selected temperature by using a furnace operating at a heating rate of 5 °C/min in a reducing environment due to 20% H_2/He flow. A Philips XL 30 scanning electron microscope (SEM) was used to investigate samples morphology surface. The crystalline structure of reduced powders was investigated by X-ray diffraction (XRD) using a Philips X-pert 3710 X-ray

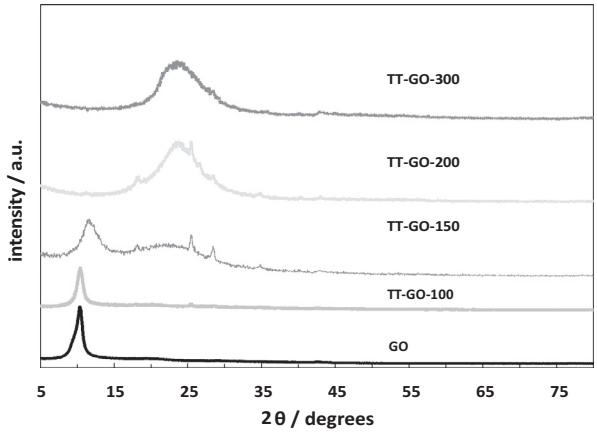

Fig. 2. XRD diffraction patterns comparison among graphene oxide (GO) and thermically treated graphene oxides (TT-GOs).

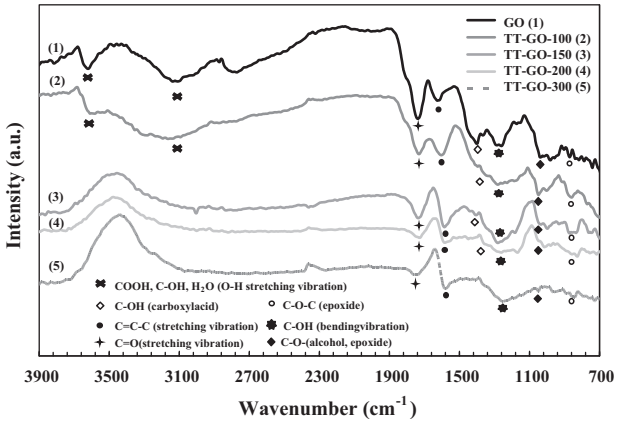

Fig. 3. FT-IR spectra of graphene oxide (GO) and thermically treated graphene oxides (TT-GOs).

diffractometer and Cu Kα radiation, operating at 40 kV and 20 mA. The peak profile of the (002) reflection associated to carbon was obtained by using the Marquardt algorithm and used to calculate the full width at half maximum (FWHM) value. The surface composition of the TT-GOs samples was investigated by X-ray photoelectron spectroscopy (XPS) using a Physical Electronics (PHI) 5800-01 spectrometer equipped with a monochromatic Al source operating at 350 W. Element spectra were acquired with pass energy of 11.75 eV. The XPS instrument was equipped with a PHI Multipack library that was further utilized to identify surface species. Each sample was separately allocated onto an aluminum-based stub and analyzed for our purposes. The oxygen-containing groups on TT-GOs surface were also investigated by Fourier-transform infrared spectroscopy FT-IR in diffuse reflectance mode (Nicolet 380 Thermo Fisher Spectrophotometer equipped). Each sample was mixed with KBr powder (10 mg TT-GOs in 300 mg KBr) then the prepared samples were collocated in an appropriate sample holder. Each measurement was performed in air collecting the signal in the range of 4000–400 cm^{-1} with a resolution of 16 cm^{-1}. 512 scans per sample were recorded and corrected against the spectrum of pure KBr as background.

2.2. Electrodes preparation

Several electrode formulations were in-house prepared by using an easy and practical method to deposit the thermically treated powders and allow to carry out cyclic voltammetry (CV) in a three electrode half-cell configuration. The wet impregnation method was utilized for the electrodes preparation. Several solutions of 10 mg of TT-GO powders dissolved in 50 ml of isopropanol (Carlo Erba, >99.5%) was preliminarily sonicated for 2 h to get a fully dispersed suspension. Afterwards, a carbon felt (CF, Freudenberg H2315, thickness: 250 μm), used as support, was impregnated with the prepared dispersion. The active area was 1.1 cm^2 for all investigated samples. A GO electrode was prepared by using the same procedure and characterized for comparison with treated samples.

2.3. Electrochemical tests

A three electrode half-cell was utilized for electrochemical characterization of all samples. A solution of 0.2 mol l^{-1} $VOSO_4$ (97 wt.% $VOSO_4 \cdot xH_2O$ Sigma-Aldrich) in 4 mol l^{-1} H_2SO_4 was used for the purpose. Potential values were measured against a saturated calomel (Hg_2/Hg_2Cl_2) reference electrode whereas Pt was used as counter electrode. The reported potential values were normalized with respect to the standard hydrogen electrode (SHE). An AUTOLAB FRA equipped Galvanostat/Potentiostat (Metrohm) was used for the electrochemical tests. Ac-impedance spectra were carried out at potential values of practical interest for application in vanadium flow batteries e.g. 1.1 V, 1.2 V and 1.25 V vs. SHE depending on the specific reversibility of the oxidation process recorded for each investigated samples. The series resistance (R_s) was determined by the high frequency intercept in the Nyquist plot.

Table 2
Oxygen atomic percentage of the graphene oxide (GO) and thermically treated graphene oxides.

Samples	C1s (%)	O1s (%)	O/C ratio
GO	70.24	29.76	0.423
TT-GO-100	71.76	28.24	0.393
TT-GO-150	74.58	25.42	0.341
TT-GO-200	80.68	19.32	0.239
TT-GO-300	84.42	15.58	0.184

3. Result and discussion

3.1. Physico-chemical characterizations

3.1.1. TG–DSC analysis

Fig. 1 shows the TG–DSC analysis carried out on a commercial GO sample in powder form. Thermogravimetric measurement allowed to individuate the weight losses due to irreversible processes of sample thermal decomposition with gasses production. As known, the functional groups can be removed by thermal reduction. The TG and DSC profile showed two (I–II) weight losses of about 15% between 100 and 150 °C due to physical and chemical dehydration, respectively. A third one (III) and higher loss (∼32%), with variation from exothermic to endothermic curve, was observed in the range 150–200 °C probably due to a significant structure morphology changes as confirmed by subsequent XRD analysis. Another evident weight loss (∼43%) was observed between 200 and 300 °C (IV) characterized by an endothermic process probably caused by the label oxygen groups decomposition. Due to the relevant weight losses, recorded for temperatures higher than 300 °C, four reduction temperatures, 100 °C, 150 °C, 200 °C and 300 °C, were selected for the GO powders synthesis in 20% H_2/He flow. Each treated sample was named as follow: TT-GO-100, TT-GO-150, TT-GO-200 and TT-GO-300.

3.1.2. XRD analysis

Fig. 2 shows a comparison among X-ray diffraction patterns of the GO and several TT-GOs samples. Analyzing the TT-GO-100 spectrum, a sharp (002) peak at $2\theta = \sim 11°$ as well as a lower full width at half maximum (FWHM) value (0.968° vs. 1.073°) was recorded (Table 1). These data were indicative of a typical AB stacked graphene oxide structure [34] characterized by a higher crystallinity with respect to the commercial GO. The little bit lower d-spacing value recorded for the sample reduced at 100 °C (Table 1) was indicative of a slight removal of the oxygen functional groups as intercalated water among layers. A structure morphology change was observed for reduced temperature higher than 100 °C, as previously observed by TG/DSC curve. A slight shift of the (002) peak to higher Bragg angles with a broadening of the FWHM value (2.504°) was recorded for the TT-GO-150 sample, as well as, an additional peak at $2\theta = \sim 24°$ appeared. The observed spectrum was indicative both of a significant vaporization of adsorbed H_2O molecules [34–36] and a gradual reduction process of the graphene oxide. The disappearing of the (002) peak at $2\theta = \sim 11°$ was evident for the TT-GO-200 sample whereas an evident peak at $2\theta = \sim 24°$ was observed. This latter was attributed to the reduced graphene oxide formation. XRD spectrum shows that the interlayer distance (Table 1) of the TT-GO-200 sample was decreased to 3.78 Å ($2\theta = 24°$) from 8.61 Å ($2\theta = 11°$) for the original commercial GO due to the elimination of the oxygen-containing groups, ascribable both to the partial removal of the main oxide groups of COOH and the removal intercalated water [34], as showed by TG/DSC measurements and further confirmed by subsequent FT-IR analysis. The XRD pattern of the TT-GO-300 sample showed a broadening of the FWHM value with respect to TT-GO-200, 5.873° vs. 5.109°, respectively, probably due to defects structure.

3.1.3. FT-IR analysis

A further investigation was carried out on the powder samples by FT-IR measurements in order to define the oxygen species on the investigated electrode surfaces. Analyzing the FT-IR transmittance spectra of the GO and TT-GO-100 samples (Fig. 3), typical peaks due to stretching mode of —OH groups in the alcohol, carboxyl, phenols form as well as water molecules were observed

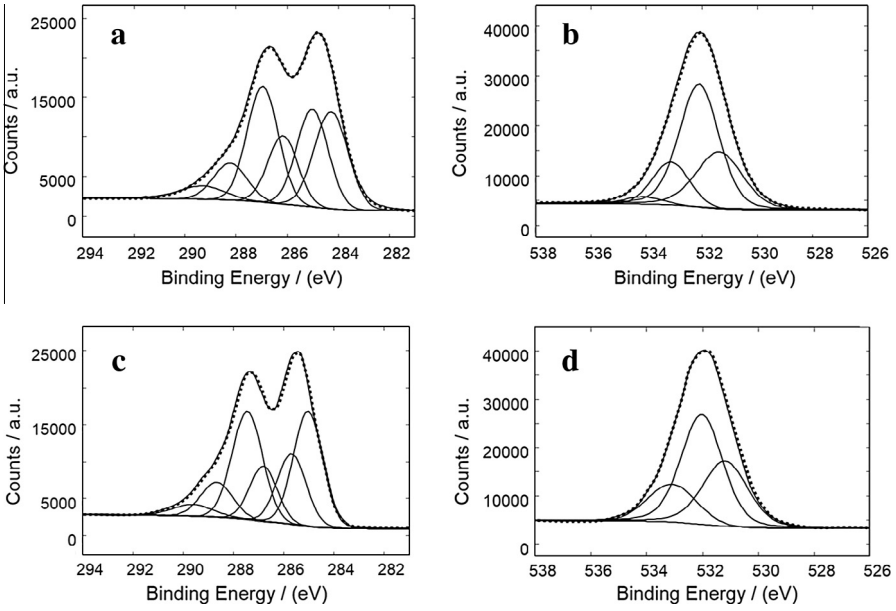

Fig. 4. XPS C1s and O1s peaks of GO (a and b), TT-GO-100 (c and d) samples.

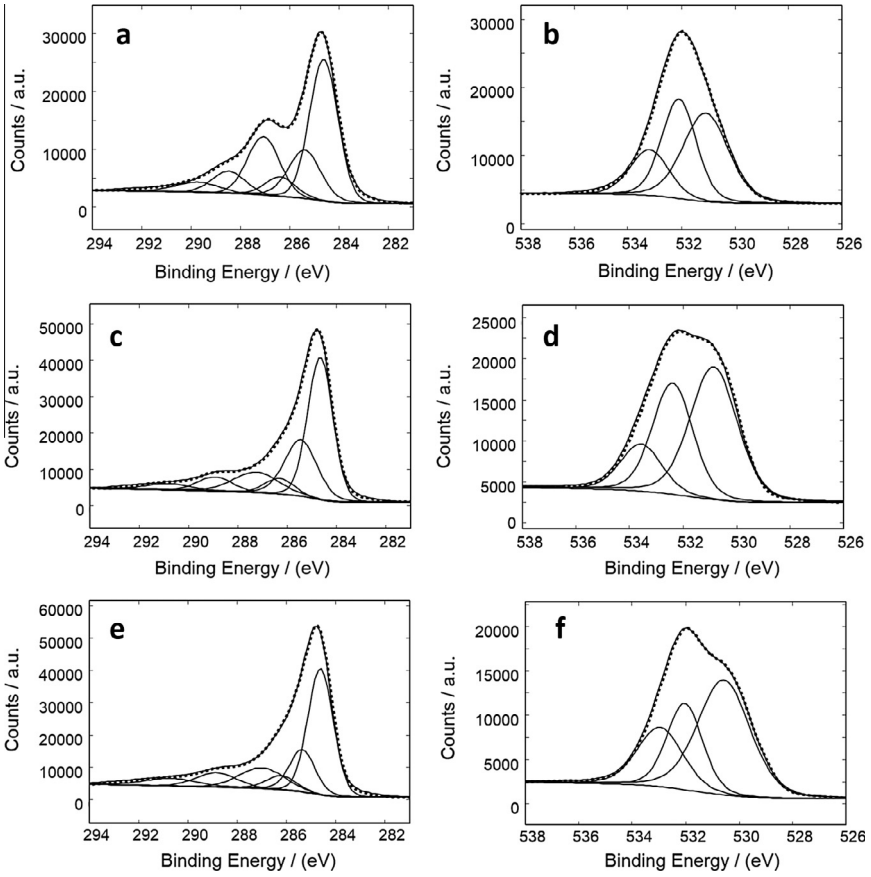

Fig. 5. XPS C1s and O1s peaks of TT-GO-150 (a and b), TT-GO-200 (c and d), TT-GO-300 (e and f) samples.

between 3700 and 2000 cm^{-1} [24]. GO and TT-GO-100 showed a further peak at ~1622 and ~1605 cm^{-1}, respectively, assigned both to the C=C—C stretch vibration (in-ring), due to the presence of aromatic groups, and adsorbed hydroxyl groups. The shift between the two peaks was indicative of the slight reduction of the peak water at 100 °C. A more intensive shift toward ~1580 cm^{-1} was observed for TT-GO-150, TT-GO-200 and TT-GO-300 samples indicating the disappearing of the adsorbed water as well as the increase of the graphitic character. All investigated samples showed the presence of C=O stretching vibration of carbonyl compound (ketone and aldehyde species) and carboxyl acid (—COOH) at ~1740 cm^{-1}. C—OH bending vibration due to carboxyl

Table 3
Functional groups resulting from curve fitting of C1s spectra (%).

Samples	C=C sp^2 (284.5 eV)	C—C sp^3 (285.5 eV)	C—OH (286.3 eV)	C—O—C (287.1 eV)	C=O (288.4 eV)	COOH (289.5 eV)
GO	24.88	22.14	13.93	25.37	9.95	3.73
TT-GO-100	31.85	18.76	12.58	23.81	9.68	3.32
TT-GO-150	51.31	9.88	6.56	19.58	9.55	3.12
TT-GO-200	59.91	8.98	4.79	16.17	7.78	–
TT-GO-300	61.35	8.59	3.07	15.95	7.36	–

Table 4
Functional groups resulting from curve fitting of O1s XPS spectra (%).

	C=O (531.03 eV)	C—OH aliphatic (532.16 eV)	C—OH phenolic (286.3 eV)	Adsorbed water
GO	30.39	52.39	15.00	2.22
TT-GO-100	32.46	52.36	15.18	–
TT-GO-150	42.13	42.55	15.32	–
TT-GO-200	46.73	33.64	19.63	–
TT-GO-300	50.04	25.23	24.73	–

species and phenolic groups (C—OH bending vibration) were recorded at ~1400 cm^{-1} and ~1280 cm^{-1}, respectively [19,32,34–36]. Moreover, peaks recorded at ~1050 cm^{-1} were attributed to alcohol and epoxide groups (C—O vibrational mode). The further peak at ~850 cm^{-1} was due to the C—O—C vibrational mode of the epoxide species. In particular, the TT-GO-100 sample showed a partial reduction of the structural —OH groups of the edge plane as well as a decrease of the carboxyl species with respect to the GO sample. A progressive and more significative decrease of the main peaks was recorded for samples treated at temperatures higher than 100 °C. FT-IR spectra of TT-GO-150, TT-GO-200 and TT-GO-300 samples (Fig. 3) showed a drastic reduction of the structural —OH groups in the range between 3700 and 2000 cm^{-1} and a more intensive decrease of the peaks at 1740 cm^{-1} indicative of a removal of carboxyl groups (—COOH) due to the reduction effect toward carbonyl species [26,34–37]. The presence of the C=C—C stretching vibration at ~1600 cm^{-1} was indicative of the graphitic domain.

3.1.4. XPS analysis

To further asses the variation of the surface atomic concentration in terms of oxygen-functional groups, XPS measurements were carried out both on the commercial GO and the TT-GO samples. A decrease of the oxygen groups percentage due to the thermal reduction was recorded (Table 2). A direct comparison of O1s and C1s curve fitting for all the samples is shown in Figs. 4 and 5. For all investigated samples, the percentage of functional groups were obtained from curve fitting of C1s and O1s spectra (Tables 3 and 4). From C1s signal deconvolution analysis, six carbon species were determined at specific Binding Energy (B.E.), i.e. graphitic carbon (C=C sp^2, 284.5 eV), hybridized carbon sp^3 (C—C 285.5 eV), hydroxyl species (C—O, 286.3 eV), epoxydic (C—O—C, 287.1 eV), carbonyl species (C=O, 288.2 eV) and carboxyl species (—COOH, 289.5 eV) [19,29,30]. Analyzing the C1s signal, a progressive percentage increase of sp^2 hybridized carbon and a consequent decrease of the sp^3 hybridized carbon was revealed passing from the GO to the TT-GO-300 sample (Table 3). Increasing reduction temperatures, a significant percentage decrease was observed for C—OH species while an increase of the carbonyl groups was revealed in correspondence of a slight carboxyl species decrease. A high and prevalent percentage of the epoxide groups was observed both for the GO and TT-GO samples. Observing Fig. 5, the TT-GO-200 and TT-GO-300 samples showed a shift of the C=O peak toward higher binding energy with respect to GO sample (288.2 vs. 288.7 eV). This shift was attributed to the COOH groups contribution in which carbonyl species were prevalent. This effect explained why the carboxyl percentage was not reported in Table 3 for temperatures higher than 150 °C. Moreover, a new peak at 290.5 eV was observed for TT-GO-200 and TT-GO-300. This latter was ascribed to the $\pi \rightarrow \pi^*$ shake-up satellite peak indicative of a typical aromatic structure [38]. A perfect percentage data relationship between the C1s and O1s signals were recorded (Table 4). In particular, the increase of the carbonyl species (C=O) was confirmed passing from GO (30.39%) to TT-GO-300 (50.04%). The presence of a little percentage of adsorbed water was revealed for the GO sample at a binding energy of 534.1 eV (2.22%). This latter disappeared for all the treated samples. A percentage decrease is observed for the C—OH aliphatic groups, ascribable to alcohol and carboxyl acid, indicating the reduction process as a function of the temperatures. On the contrary, an evident and more effective increase of the phenolic groups (C—OH) was observed passing from the GO and TT-GO-100 to the TT-GO-300 sample, ~15% vs. ~24%, respectively. The presence of C—O—C and C—OH groups, close together on the basal plane, could favors the formation of phenolic groups by increasing reduction temperatures. All the obtained results were in accordance with the FT-IR spectra data.

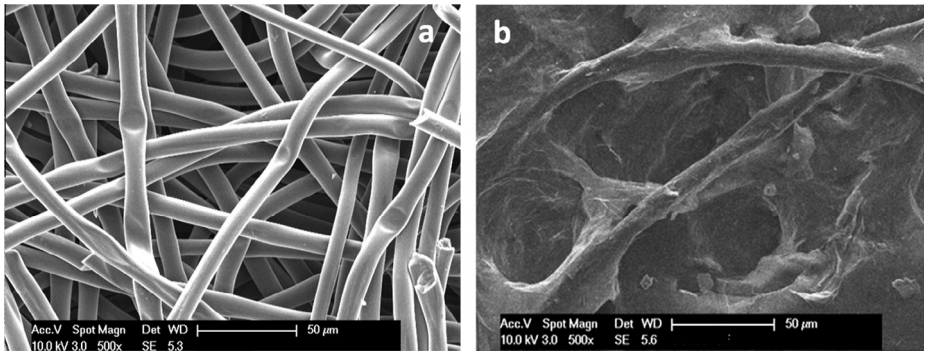

Fig. 6. SEM images of CF support before (a) and after wet impregnation of the TT-GO-150 sample (b).

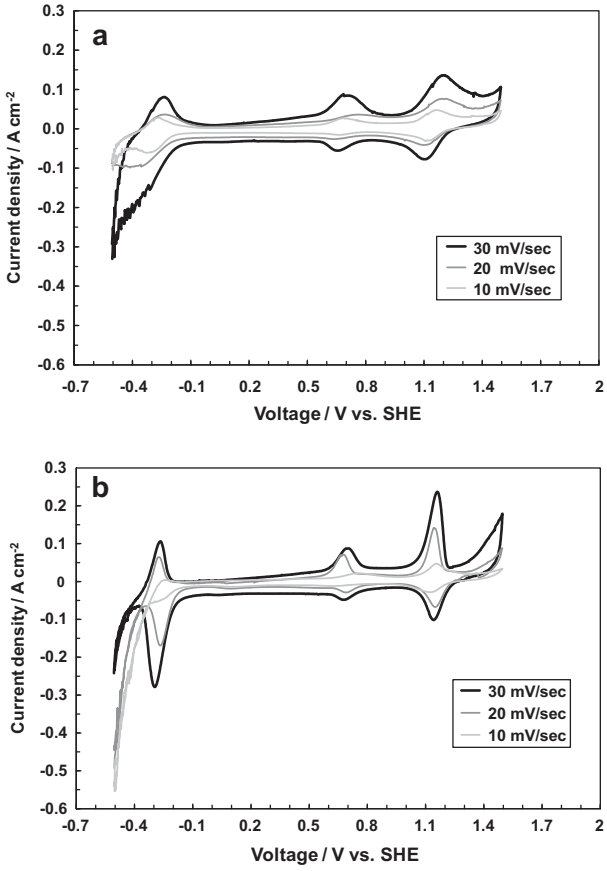

Fig. 7. CV curves of GO (a), TT-GO-100 (b) electrodes in 0.2 M $VOSO_4$ + 4 M H_2SO_4 solution at different scan rate.

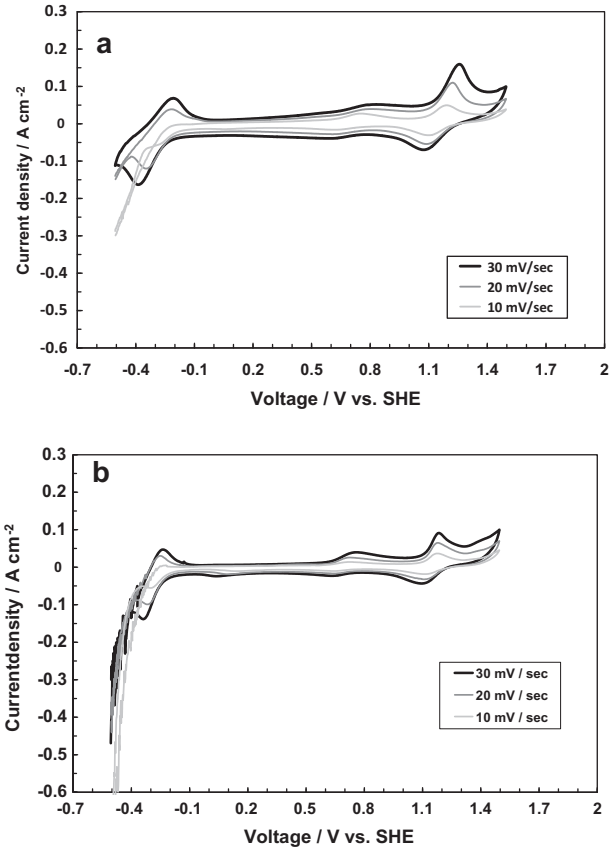

Fig. 8. CV curves of TT-GO-150 (a), TT-GO-200 (b) and TT-GO-300 (c) electrodes in 0.2 M $VOSO_4$ + 4 M H_2SO_4 solution at different scan rate.

3.2. Electrochemical characterizations

The correlation between the physico-chemical behaviors and electrochemical performance of the several samples was investigated by cyclic voltammetry and electrochemical impedance spectroscopy. The CV curves were carried out on the electrodes prepared by wet impregnation of the CF support by using a well dispersed solution containing the investigated samples. The homogenous deposition of each sample on the support was confirmed by SEM analysis; a SEM image of TT-GO-150 dispersion, before and after the wet impregnation deposition, is shown in Fig. 6 as example for the purpose. Figs. 7(a–b), 8(a–b) and 9 show CV curves for commercial GO and TT-GO electrodes at different scan rates in a 0.2 M $VOSO_4$ + 4 M H_2SO_4 solution. All the electrochemical parameters were listed in Table 5. As better observed in Fig. 10, the TT-GO-100 exhibited the higher electrocatalytic activity toward the cathodic redox reaction $[VO]^{2+}/[VO_2]^{+}$ showing a redox peak potential at 1.16 V and 1.13 V as well as the highest redox current density value (Table 5). The oxidation and reduction peaks of V^{2+}/V^{3+} (−0.26 V and −0.3 V) and V^{3+}/V^{4+} (0.7 V and 0.67 V) were indicative of the higher reversibility of the processes on the electrode surface interface for the anode reaction. Moreover, the highest on-set potential value of the oxidation (at 1.05 V) was indicative of a better kinetic reaction with respect the other electrode samples. The prevalence of hydroxyl and carboxyl species favor the enhancement of the adsorption of vanadium ion species on the electrode surface improving the electrode reaction kinetic. A lower electrocatalytic activity toward the above indicated processes was recorded for the other electrode samples (Table 5). Although the TT-GO-150 electrode showed a good kinetic

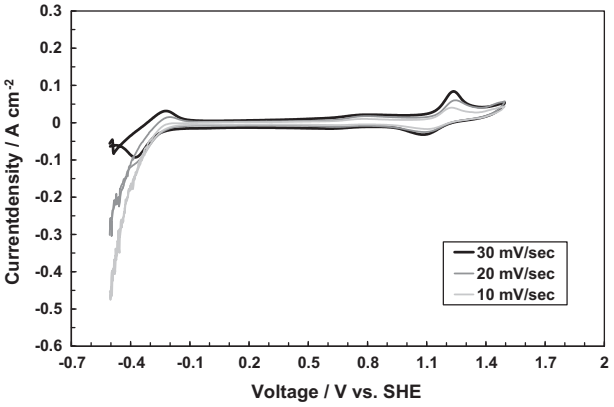

Fig. 9. CV curves of TT-GO-300 (a) electrode in 0.2 M $VOSO_4$ + 4 M H_2SO_4 solution at different scan rate.

reversibility toward the oxidation/reduction vanadium processes, this latter was lower compared with the GO and TT-GO-100 electrodes performance, showing a peak to peak separation of 0.19 V vs. 0.06 V and 0.03 V, respectively. TT-GO-150 electrode electrochemical result was in accordance with the higher oxygen species presence on the electrode surface (25.42%, Table 2) mainly ascribed to carbonyl and phenolic groups as well as to the partial structure morphology change (Fig. 1). Analyzing the TT-GO-200 CV profile, a drastic reduction of the current density intensity was recorded as well as a lower reversibility with respect to the treated graphene oxide at 100 °C. TT-GO-300 electrode exhibited the worst performance (Fig. 9) in terms of peak current density value as well as

Table 5
Electrochemical parameter from CV curves of the graphene oxide (GO) and thermically reduced graphene oxides.

Samples	E_a (V)	E_c (V)	ΔE (V)	I_{pa}/I_{pc}
GO	1.20	1.14	0.06	2.88
TT-GO-100	1.16	1.13	0.03	2.05
TT-GO-150	1.26	1.07	0.19	2.21
TT-GO-200	1.19	1.08	0.11	2.11
TT-GO-300	1.25	1.08	0.17	2.53

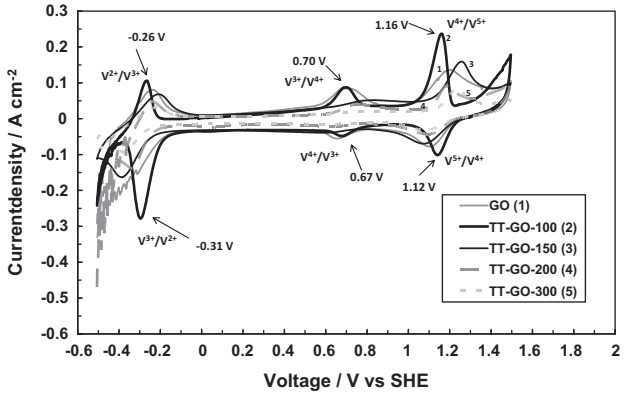

Fig. 10. Comparison among CV curves of all the investigated electrodes in a 0.2 M $VOSO_4$ + 4 M H_2SO_4 solution at a scan rate of 30 mV sec^{-1}.

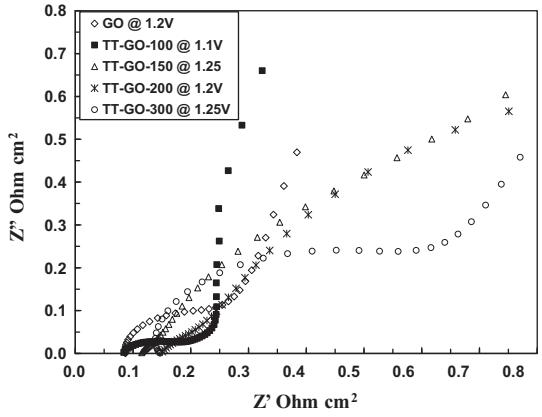

Fig. 11. Nyquist plots comparison among GO (at 1.2 V), TT-GO-100 (at 1.1 V), TT-GO-150 (at 1.25 V), TT-GO-200 (at 1.2 V) and TT-GO-300 (at 1.25 V) electrodes.

reversibility. The low recorded electrochemical performance was caused by the increase of the electron resistance for both electrodes due to the prevalent contribution attributable to the high epoxide groups percentage (~16%) and phenol species percentage (~20%), as revealed by physico-chemical data. This clarify how these functional groups are not involved as active sites in the vanadium redox reactions. EIS curves (Fig. 11) showed a small series resistance value (R_s) both for the GO (0.084 ohm cm^2) and the treated GO at 100 °C (0.086 ohm cm^2) indicative of a hydrophilic surface due to the presence of hydroxyl species. GO and TT-GO-100 electrodes showed a Nyquist plots characterized by an R_{ct} ~0.19 ohm cm^2 and ~0.11 ohm cm^2 at 1.2 V and 1.1 V, respectively, indicating the faster reaction at the electrode/electrolyte interface for the sample treated at 100 °C. This latter result confirmed the higher electrocatalytic activity recorded for the TT-GO-100 electrode with respect to the other samples. Higher R_s values were recorded for the TT-GO-150, TT-GO-200 and TT-GO-300 electrodes, 0.11 ohm cm^2, 0.145 ohm cm^2 and 1.47 ohm cm^2, respectively, confirming the decreasing of the electrodes wettability. An R_{ct} value of about 0.6 ohm cm^2 was recorded for the TT-GO-300 sample in accordance with the lower electrochemical performance. Thus ac-impedance data reinforced the electrochemical performance results.

4. Conclusions

An in-depth investigation of in-house thermically treated graphene oxide electrochemical properties, as a function of the oxygen functional groups, was carried out by developing electrodes prepared by wet impregnation method in which carbon felt was used as a support for the purpose. The TT-GO-100 showed the better electrocatalytic activity mainly attributed both to the higher crystalline structure with respect to the GO sample and to the prevalent hydroxyl and carboxyl species content with respect to the other treated samples. These oxygen species were responsible of the electron resistance reduction in favor of an reaction kinetic enhancement proving their fundamental role as active sites both for the $[VO]^{2+}/[VO_2]^{+}$ and V^{2+}/V^{3+} redox reaction processes. The TT-GO-150, TT-GO-200 and TT-GO-300 samples, characterized by a more graphitic structure due to the reduced graphene oxide structure formation, showed a decrease of the electrical conduction on the electrode surface mainly correlated to the presence of a high percentage of epoxide and phenolic groups on the basal plane responsible of the high ohmic and charge transfer resistance. Thanks to the development of electrodes characterized by a high mechanical strength due to the CF properties as well as a high electrocatalytic activity, due to the impregnated graphene oxide, was possible to investigate and individuate an effective anode and cathode electrode in the perspective of a large area MEA scale-up for battery configuration of practical interest.

Acknowledgement

Authors from CNR-ITAE acknowledge the financial support from "Ministero dello Sviluppo Economico – Accordo di Programma MSE-CNR per la Ricerca del Sistema elettrico Nazionale".

References

[1] Rahman F, Skyllas-Kazacos M. Solubility of vanadyl sulfate in concentrated sulfuric acid solutions. J Power Sources 1998;72:105–10.
[2] Vijayakumar M, Burton SD, Huang C, Li L, Yang Z, Graffa GL, et al. Nuclear magnetic resonance studies on vanadium(IV) electrolyte solutions for vanadium redox flow battery. J Power Sources 2010;195:7709–17.
[3] Rahman F, Skyllas-Kazacos M. Vanadium redox battery: positive half-cell electrolyte studies. J Power Sources 2009;189:1212–9.
[4] Skyllas-Kazacos M, Rychcik M, Robbins RG, Fane AG, Green M. New all vanadium redox flow cell. J Electrochem Soc 1986;113:1057–8.
[5] Teng X, Zhao Y, Xi J, Wu Z, Qiu X, Chen L. Nafion/organically modified silicate hybrids membrane for vanadium redox flow battery. J Power Sources 2009;189:1240–6.
[6] Joerissen L, Garche J, Fabjan Ch, Tomazic G. Possible use of vanadium redox flow batteries for energy storage in small grids and stand-alone photovoltaic systems. J Power Sources 2004;127:98–104.
[7] Rydh CJ. Environmental assessment of vanadium redox and lead–acid batteries for stationary energy storage. J Power Sources 1999;80:21–9.
[8] Oriji G, Katayama Y, Miura T. Investigations on V(IV)/V(V) and V(II)/V(III) redox reactions by various electrochemical methods. J Power Sources 2005;139:321–4.
[9] Yao C, Zhang H, Liu T, Li X, Liu Z. Carbon paper coated with supported tungsten trioxide as novel electrode for all-vanadium flow battery. J Power Sources 2012;218:455–61.
[10] Vazquez S, Srdjan M, Lukic S-M, Galvan E, Franquelo L-G, Carrasco J-M. Energy storage systems for transport and grid applications. IEEE Trans Industr Electron 2010;57:3881–95.
[11] Xiong F, Zhou D, Xie Z, Chen Y. A study of the Ce^{3+}/Ce^{4+} redox couple in sulfamic acid for redox battery application. Appl Energy 2012;99:291–6.

[12] Mulder G, Six D, Claessens B, Broes T, Omar N, Van Mierlo J. The dimensioning of PV-battery system depending on the incentive and selling price conditions. Appl Energy 2013;111:1126–35.
[13] Kim S, Yan J, Schwenzer B, Zhang J, Li L, Liu J, et al. Cycling performance and efficiency of sulfonated poly(sulfone) membranes in vanadium redox flow batteries. Electrochem Commun 2010;12:1650–3.
[14] Landgrebe AR, Donley SW. Battery storage in residential applications of energy from photovoltaic sources. Appl Energy 1983;15:127–37.
[15] Hu X, Murgovski N, Johannesson L-M, Egardtn B. Comparison of three electrochemical energy buffers applied to a hybrid bus powertrain with simultaneous optimal sizing and energy management. IEEE Trans Intell Transport Syst 2014;15:1193–205.
[16] Dunn B, Kamath H, Tarascon J-M. Electrical energy storage for the grid: a battery of choices. Science 2011;334(6058):928–35.
[17] Di Blasi A, Briguglio N, Di Blasi O, Antonucci V. Charge–discharge performance of carbon fiber-based electrodes in a single cell and short stack for vanadium redox flow battery. Appl Energy 2014;125:114–22.
[18] Zhao P, Zhang H, Zhou H, Yi B. Nickel foam and carbon felt applications for sodium polysulfide/bromine redox flow battery electrodes. Electrochim Acta 2005;51:1091–8.
[19] Di Blasi A, Di Blasi O, Briguglio N, Aricò AS, Sebastiàn D, Làzaro MJ, et al. Investigation of several graphite-based electrodes for vanadium redox flow cell. J Power Sources 2013;227:15–23.
[20] Shao Y, Wang X, Engelhard M, Wang C, Dai S, Liu J, et al. J Power Sources 2010;195:4375–9.
[21] Li W, Liu J, Yan C. The electrochemical catalytic activity of single-walled carbon nanotubes towards VO_2^+/VO^{2+} and V^{3+}/V^{2+} redox pairs for an all vanadium redox flow battery. Electrochem Acta 2012;79:102–8.
[22] Zhang W, Xi J, Li Z, Zhou H, Liu L, Wu Z, et al. Electrochemical activation of graphite felt electrode for VO^{2+}/VO_2^+ redox couple application. Electrochim Acta 2013;89:429–35.
[23] Flox C, Skoumal M, Rubio-Garcia J, Andreu T, Ramon Morante J. Strategies for enhancing electrochemical activity of carbon-based electrodes for all-vanadium redox flow batteries. Appl Energy 2013;109:344–51.
[24] Yue L, Li W, Sun F, Zhao L, Xing L. Highly hydroxylated carbon fibres as electrode materials of all-vanadium redox flow battery. Carbon 2010;48:3079–90.
[25] Mohammadi T, Chieng SC, Skyllas Kazacos M. Water transport study across commercial ion exchange membranes in the vanadium redox flow battery. J Membr Sci 1997;133:151–9.
[26] Zhou JH, Sui ZJ, Zhu J, Li P, Chen D, Dai YC, et al. Characterization of surface oxygen complexes on carbon nanofibers by TPD, XPS, and FT-IR. Carbon 2007;45(4):785–96.
[27] Li W, Liu J, Jan Ch. Graphite-graphite oxide composite electrode for vanadium redox flow battery. Electrochem Acta 2011;56:5290–4.
[28] Zhang G, Sun S, Yang D, Dodelet JP, Sacher E. The surface analytical characterization of carbon fibers functionalized by H_2SO_4/HNO_3 treatment. Carbon 2008;46:196.
[29] Novoselov KS, Fal'ko VI, Colombo L, Gellert PR, Schwab MG, Kim K. A roadmap for graphene. Nature 2012;490:192–200.
[30] Du AJ, Zhu ZH, Smith SC. Multifunctional porous graphene for nanoelectronics and hydrogen storage: new properties revealed by first principle calculations. J Am Chem Soc 2010;132:2876–7.
[31] Luo B, Liu SM, Zhi LJ. Chemical approaches toward graphene-based nanomaterials and their applications in energy-related areas. Small 2012;8:630–46.
[32] Han P, Wang H, Liu Z, Chen X, Ma W, Yao J, et al. Graphene oxide nanoparticles as excellent electrochemical active materials for VO_2^+/VO^{2+} and V^{2+}/V^{3+} redox couples for a vanadium redox flow battery. Carbon 2011;49:693–700.
[33] Gonzàlez Z, Botas C, Blanco C, Santamarìa R, Granda M, Alvarez P, et al. Graphite oxide-based graphene materials as positive electrodes in vanadium redox flow batteries. J Power Sources 2013;241:349–54.
[34] Ju H-M, Huh SH, Choi S-H, Lee H-L. Structures of thermally and chemically reduced graphene. Mater Lett 2010;64:357–60.
[35] Hontoria-Lucas C, Lopezpeinado AJ, Lopez-Gonzalez JDD, Rojas-Cervantes ML, Martin-Aranda RM. Study of a oxygen-containing groups in a series of graphite oxides: physical and chemical characterization. Carbon 1995;33:1585–92.
[36] Gao C, Wang NF, Peng S, Liu SQ, Lei Y, Liang XX, Zeng SS, Zi HF. Influence of Fenton's reagent treatment on electrochemical properties of graphite felt for all vanadium redox flow battery. Electrochim Acta 2013;88:193–202.
[37] Skyllas-Kazacos M, Sun B. Chemical modification of graphite electrode materials for vanadium redox flow battery application-II. Thermal treatment. Electrochim Acta 1992;37:1253.
[38] Mattevi C, Eda G, Agnoli S, Miller S, Mkhoyan KA, Celk O, Mastrogiovanni D, Granozzi G, Garfunkel E, Chhowalla M. Evolution of electrical, chemical, and structural properties of transparent and conducting chemically derived graphene thin films. Adv Funct Mater 2009;19:2577–83.